Quantum interferences in four-wave mixing processes inside a cavity driven by quantized fields*

Li Peng-Bo(李蓬勃)†

Department of Applied Physics, Xi'an Jiaotong University, Xi'an 710049, *China*

(Received 8 July 2010; revised manuscript received 17 January 2011)

Interferences in the quantum fluctuations of the output fields are demonstrated in four-wave mixing processes inside a cavity, which is driven by two quantized fields at the signal and the idler frequencies. These interferences depend on the phase fluctuations of the input fields and induce mode splitting in the transmission spectra.

Keywords: quantum interferences and coherence, four-wave mixing

PACS: 42.50.Lc, 42.50.Gy, 42.65.–k **DOI:** 10.1088/1674-1056/20/5/054202

1. Introduction

Quantum interference and quantum coherence effects have been well studied in recent years and are central to determining the optical properties of quantum systems.[1,2] In coherently prepared atomic systems, electromagnetically induced transparency (EIT) plays a leading role,[3,4] which has been utilized in a variety of applications, such as enhanced nonlinear optics,[5,6] laser cooling,[7] quantum memory,[8,9] quantum computation and quantum communication.[10,11] Physically, the EIT is based on the destructive quantum interferences of the two adjacent atomic transitions in a typical Λ configuration atomic system. It has been recently realized that quantum interferences occur not only in multilevel systems driven by coherent fields, but also in nonresonant systems, such as an optical parametric amplifier (OPA).[12−14] It is well known that parametric interactions generate fields which have important quantum properties.[15] In the case of the classical parametric interactions in a cavity, a variety of interference effects have been observed when the cavity is driven by a field at the signal frequency.[12] The interferences arise from the signal field at the input and that generated by the pump field. In a recent letter,[13] the interferences which are initiated due to input quantized fields at the signal frequency, especially interferences in the quantum fluctuations of the output of an OPA, are reported.

In this study, we investigate the quantum interference phenomena in four-wave mixing processes inside a cavity,[16,17] which is driven by two quantized fields at the signal and the idler frequencies respectively. By utilizing the input–output formulation of the optical cavities,[18] we demonstrate the interferences in the quantum fluctuations of the two output fields. These interference effects depend on the phase fluctuations of the input fields and lead to mode splitting in the transmission spectra. In contrast to the results obtained in Ref. [13], we find here a novel cross mode modulation phenomenon, i.e., the spectrum profile for one field can be controlled by varying the parameters of the other field. Under certain conditions, the EIT-like two-peak shape of the spectrum profile can be obtained. The quadrature phase fluctuation spectra for two-mode fields are also utilized to demonstrate the interferences at the output,[19] which displays some different features comparing to Ref. [13]. These cross mode modulation phenomena arise not only from the input field and the produced field, but also from the two input fields themselves. These interference effects can help us to deeply understand the physics of quantum interference and quantum coherence in optical systems.

2. Model and method

We consider the four-wave mixing processes in a two-mode cavity with 100% reflecting left mirror and partially reflecting right mirror, as sketched in Fig. 1.

*Project supported by the New Staff Research Support Plan of Xi'an Jiaotong University, China (Grant No. 08141015).

†Corresponding author. E-mail: lipengbo@mail.xjtu.edu.cn

© 2011 Chinese Physical Society and IOP Publishing Ltd

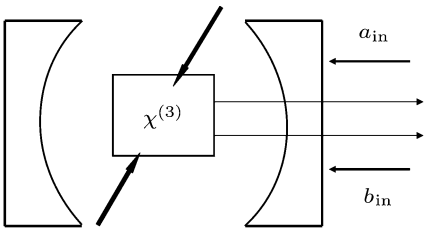


Fig. 1. Schematic diagram of four-wave mixing in a cavity.

Two classical pump fields with frequencies ν_1 and ν_2 interact with a third-order nonlinear optical material, generating the quantized signal and idler fields with frequencies ω_1 and ω_2. The cavity resonance frequencies are $\omega_{\rm a}$ and $\omega_{\rm b}$. We assume that the cavity is also driven by two quantum fields $\hat{a}_{in}$ and $\hat{b}_{in}$ with respect to the two cavity fields. We focus on the new features arising from the quantum nature of the input fields $\hat{a}_{\rm in}$ and $\hat{b}_{\rm in}$.[13] In the interaction picture and a frame rotating with the frequencies of the signal and the idler fields, the Hamiltonian describing the four-wave mixing processes is (let $\hbar = 1$)

$$H_{\rm I} = \Delta_1 \hat{a}^\dagger \hat{a} + \Delta_2 \hat{b}^\dagger \hat{b} + G\hat{a}\hat{b} + G^* \hat{a}^\dagger \hat{b}^\dagger, \qquad (1)$$

where $\hat{a}$ and $\hat{b}$ are the annihilation operators for the signal and the idler fields, respectively. The detunings are $\Delta_1 = \omega_1 - \omega_{\rm a}$ and $\Delta_2 = \omega_2 - \omega_{\rm b}$. The coupling parameter $G = \chi^{(3)} E_1 E_2$, where $\chi^{(3)}$ is the third-order susceptibility, E_1 and E_2 are the amplitudes of the pump fields. For simplicity, we assume G to be real in the following discussion. Physically, four-wave mixing in a cavity can be achieved through two-, three- or four-level atoms[16,20,21] dispersively interacting with two nondegenerate cavity modes pumped by two classical fields with amplitudes of E_1 and E_2. Under certain conditions, one can obtain the interaction Hamiltonian of the Eq. (1) form, with the coupling strength G depending on the relevant frequency detuning and pump field intensity.[20,21] To be more specific, we consider four wave mixing with two-level atoms in a two-mode optical cavity.[20] The atomic ground state $|g\rangle$ and the excited state $|e\rangle$, with transition frequency ω_0, are coupled through the cavity modes of frequencies $\omega_{\rm a}$ and $\omega_{\rm b}$, with coupling strengths $g_{\rm a}$ and $g_{\rm b}$, and detunings $\delta_{\rm a} = \omega_0 - \omega_{\rm a}$ and $\delta_{\rm b} = \omega_0 - \omega_{\rm b}$. The dipole-allowed transition $|g\rangle \leftrightarrow |e\rangle$ is also pumped by two driving classical fields of frequencies ν_1 and ν_2, with coupling constants Ω_1 and Ω_2,and detunings $\delta_1 = \omega_0 - \nu_1$ and $\delta_2 = \omega_0 - \nu_2$. In the interaction picture, the Hamiltonian is given by $H_{\rm I} = g_{\rm a} {\rm e}^{{\rm i}\,\delta_{\rm a} t} \hat{a}\sigma_{\rm eg} + g_{\rm b} {\rm e}^{{\rm i}\,\delta_{\rm b} t} \hat{b}\sigma_{\rm eg} + (\Omega_1 {\rm e}^{{\rm i}\,\delta_1 t} + \Omega_2 {\rm e}^{{\rm i}\,\delta_2 t})\sigma_{\rm eg} + {\rm H.c.}$, with $\sigma_{\rm eg} = |e\rangle\langle g|$. Following the derivation given in Ref. [20], one can get the Hamiltonian $(\hat{a}\hat{b} + {\rm H.c.})$, with the coupling constant $G = g_{\rm a} g_{\rm b} \Omega_1^2 / (\delta^2 - 4\Omega_1^2)$, where $\delta_{\rm a} = -\delta_{\rm b} = \delta > 0$.

We consider the input–output theory and suppose that each cavity mode interacts independently with the respective input field.[22] Then in the Markov approximation, we obtain the following coupled equations for the quantized fields inside the cavity:

$$\frac{{\rm d}\hat{a}}{{\rm d}t} = -{\rm i}\,\Delta_1 \hat{a} - {\rm i}\,G\hat{b}^\dagger - \kappa_a \hat{a} + \sqrt{2\kappa_a}\hat{a}_{\rm in}, \qquad (2a)$$

$$\frac{{\rm d}\hat{b}}{{\rm d}t} = -{\rm i}\,\Delta_2 \hat{b} - {\rm i}\,G\hat{a}^\dagger - \kappa_b \hat{b} + \sqrt{2\kappa_b}\hat{b}_{\rm in}, \qquad (2b)$$

where κ_a and κ_b are the cavity decay rates of mode a and mode b. The output fields are given by

$$\hat{a}_{\rm out} + \hat{a}_{\rm in} = \sqrt{2\kappa_a}\hat{a}, \qquad (3a)$$

$$\hat{b}_{\rm out} + \hat{b}_{\rm in} = \sqrt{2\kappa_b}\hat{b}. \qquad (3b)$$

Equations (2) and (3) can be solved by performing the Fourier transformation from the time domain to the frequency domain. Then we get the following results

$$\hat{a}_{\rm out}(\omega) = A_1 \hat{a}_{\rm in}(\omega) - B_1 \hat{b}_{\rm in}^\dagger(-\omega), \qquad (4a)$$

$$\hat{b}_{\rm out}(\omega) = A_2 \hat{b}_{\rm in}(\omega) - B_2 \hat{a}_{\rm in}^\dagger(-\omega), \qquad (4b)$$

where

$$A_1 = \frac{2\kappa_a(-{\rm i}\,\omega - {\rm i}\,\Delta_2 + \kappa_b)}{(-{\rm i}\,\omega - {\rm i}\,\Delta_2 + \kappa_b)(-{\rm i}\,\omega + {\rm i}\,\Delta_1 + \kappa_a) - G^2} - 1, \qquad (5a)$$

$$B_1 = \frac{2\sqrt{\kappa_a \kappa_b}\,{\rm i}\,G}{(-{\rm i}\,\omega - {\rm i}\,\Delta_2 + \kappa_b)(-{\rm i}\,\omega + {\rm i}\,\Delta_1 + \kappa_a) - G^2}, \qquad (5b)$$

$$A_2 = \frac{2\kappa_b(-{\rm i}\,\omega - {\rm i}\,\Delta_1 + \kappa_a)}{(-{\rm i}\,\omega - {\rm i}\,\Delta_1 + \kappa_a)(-{\rm i}\,\omega + {\rm i}\,\Delta_2 + \kappa_b) - G^2} - 1, \qquad (5c)$$

$$B_2 = \frac{2\sqrt{\kappa_a \kappa_b}\,{\rm i}\,G}{(-{\rm i}\,\omega - {\rm i}\,\Delta_1 + \kappa_a)(-{\rm i}\,\omega + {\rm i}\,\Delta_2 + \kappa_b) - G^2}. \qquad (5d)$$

To get more insight into the four-wave mixing processes, we can define the spectral matrix for the output fields as

$$\langle \hat{\boldsymbol{a}}_i(t)\hat{\boldsymbol{a}}_j(t+\tau)\rangle = \frac{1}{2\pi}\int S_{ij}^{\rm out}(\omega)\mathrm{e}^{-\mathrm{i}\,\omega\tau}\mathrm{d}\omega, \quad (6a)$$

$$\langle \hat{\boldsymbol{a}}_i(\omega')\hat{\boldsymbol{a}}_j(\omega)\rangle = 2\pi\delta(\omega'-\omega)S_{ij}^{\rm out}(\omega), \quad (6b)$$

where $(i,j=1,2,3,4)$; $\hat{\boldsymbol{a}} = (\hat{a}_{\rm out}^{\dagger}, \hat{a}_{\rm out}, \hat{b}_{\rm out}^{\dagger}, \hat{b}_{\rm out})$. The elements $S_{12}^{\rm out}(\omega)$ and $S_{34}^{\rm out}(\omega)$ determine the intensity fluctuations in the output fields, while $S_{24}^{\rm out}(\omega)$ determines the phase dependent properties (i.e., squeezing) of the output fields.

We assume that the input fields are two-mode squeezed fields. This gives the following expectation values:

$$\langle \hat{a}_{\rm in}^{\dagger}(\omega')\hat{a}_{\rm in}(\omega)\rangle = 2\pi\delta(\omega'-\omega)\alpha, \quad (7a)$$

$$\langle \hat{b}_{\rm in}^{\dagger}(\omega')\hat{b}_{\rm in}(\omega)\rangle = 2\pi\delta(\omega'-\omega)\alpha, \quad (7b)$$

$$\langle \hat{a}_{\rm in}(\omega')\hat{b}_{\rm in}(\omega)\rangle = -2\pi\delta(\omega'-\omega)\beta\mathrm{e}^{\mathrm{i}\,\theta}, \quad (7c)$$

where $\alpha = \sinh^2\zeta$, $\beta = \sinh\zeta\cosh\zeta$ and the squeezing parameter $\xi = \zeta\mathrm{e}^{\mathrm{i}\,\theta}$. From Eqs. (4)–(7), we can calculate the spectra $S_{\rm a}^{\rm out} \equiv S_{12}^{\rm out}(\omega)$ and $S_{\rm b}^{\rm out} \equiv S_{34}^{\rm out}(\omega)$, which are given by

$$S_{\rm a}^{\rm out}(\omega) = \beta|A_1 + \mathrm{e}^{\mathrm{i}\,\theta}B_1|^2 + (\alpha-\beta)|A_1|^2 + (\alpha-\beta+1)|B_1|^2, \quad (8a)$$

$$S_{\rm b}^{\rm out}(\omega) = \beta|A_2 + \mathrm{e}^{\mathrm{i}\,\theta}B_2|^2 + (\alpha-\beta)|A_2|^2 + (\alpha-\beta+1)|B_2|^2. \quad (8b)$$

Equation (8) gives one of our central results in this work. Define the quadrature operator $X = \frac{1}{\sqrt{2}}(\hat{a} + \hat{b} + \hat{a}^{\dagger} + \hat{b}^{\dagger})$, then one can calculate the quadrature phase fluctuation spectrum at the output,

$$V(X^{\rm out}) = S_{12}^{\rm out} + S_{34}^{\rm out} + S_{24}^{\rm out} + S_{24}^{\rm out*} + \frac{1}{2}(|A_1|^2 - |B_1|^2 + A_1B_2 - A_2B_1 + A_1^*B_2^* - A_2^*B_1^*), \quad (9)$$

which gives another central result of this study. We will use these results to show a variety of quantum interference and quantum coherence phenomena. A similar form of Eq. (8) has been obtained by Agarwal[13] in the case of the degenerate parametric amplifier. In this work we will show some different quantum interference effects. An obvious difference between the results of this work and that of Ref. [13] is that the spectrum for one output field depends on the parameters of both input fields in this work, whereas in Ref. [13] the output spectrum is solely determined by one input field. We note from Eq. (4) that mean field $\langle \hat{a}_{\rm out}(\omega)\rangle \neq 0$ (or $\langle \hat{b}_{\rm out}(\omega)\rangle \neq 0$), even the initial quantum field is such that $\langle \hat{a}_{\rm in}(\omega)\rangle = 0$ (or $\langle \hat{b}_{\rm in}(\omega)\rangle = 0$). Other different results are the spectra $S_{24}^{\rm out}(\omega)$ and $S_{42}^{\rm out}(\omega)$, which can be calculated from the above equations,

$$S_{24}^{\rm out}(\omega) = -\beta(A_1A_2\mathrm{e}^{\mathrm{i}\,\theta} + B_1B_2\mathrm{e}^{-\mathrm{i}\,\theta}) - A_1B_2\eta - A_2B_1\alpha, \quad (10a)$$

$$S_{42}^{\rm out}(\omega) = -\beta(A_1A_2\mathrm{e}^{\mathrm{i}\,\theta} + B_1B_2\mathrm{e}^{-\mathrm{i}\,\theta}) - A_2B_1\eta - A_1B_2\alpha, \quad (10b)$$

where $\eta = \cosh^2\zeta$. The phase fluctuations in the squeezed input fields at the signal and the idler frequencies allow the two terms in Eq. (4) to beat, thus leading to interferences. These interferences are functions of ω, two detunings Δ_1, Δ_2, the coupling parameter G and the squeezing parameter ξ of the input fields. In the following discussions, we will show a variety of the interference effects.

We first investigate the detuning dependence of the fluctuation spectrum for the signal field at $\omega = 0$. In the following discussions we assume that the cavity decay rates for the signal and the idler fields are the same $\kappa_a = \kappa_b = \kappa$ and choose all the parameters in unit of κ. Figure 2 shows the behaviour of $S_{\rm a}^{\rm out}(0)$ versus the signal detuning Δ_1 at different values of θ and idler detuning Δ_2. All the output spectra are normalized to the output spectra for $G = 0$. In Fig. 2(a), we let $\theta = -\pi/2$ and plot the signal output spectrum as a function of detuning Δ_1 under five different values of idler detuning Δ_2, i.e., $\Delta_2/\kappa = -5, -3, 0, 3, 5$. We observe mode splitting when $\Delta_1 = \Delta_2 = 0$. The origin of mode splitting in the output spectra of four-wave mixing is the destructive interference. Another obvious phenomenon is that the idler detuning greatly influences the spectrum of the signal field. At different idler detunings, the spectrum profiles of the signal output field are different even at the same θ. Therefore, one can control the spectrum profile for one field by varying the detuning of the other field. In Figs. 2(b)–2(c), we consider the spectrum versus the detunings in the situations $\theta = -3\pi/4$ and 0. Quantum interferences in the fluctuations of the output can also be clearly seen.

Next we consider the behaviour of $S_{\rm a}^{\rm out}(\omega)$ as a function of angular frequency ω at different values

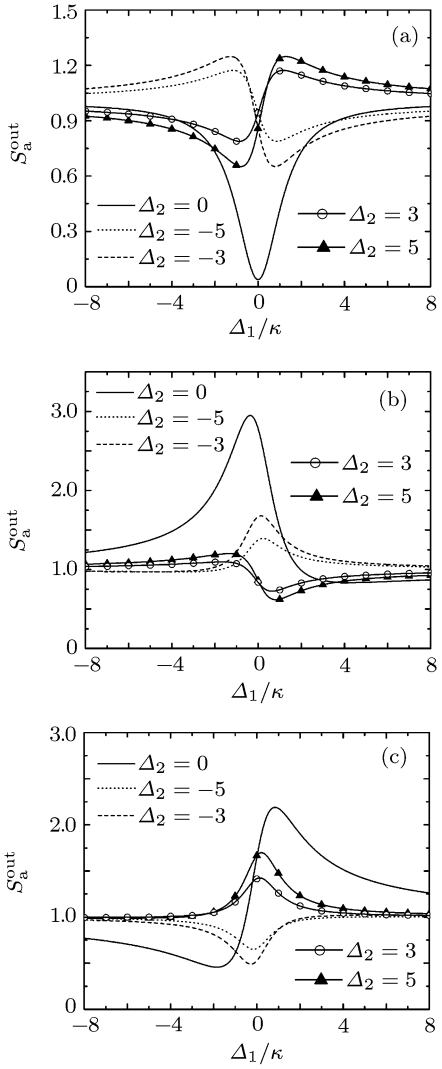


Fig. 2. The fluctuation spectra of the signal field in the output vs the detuning Δ_1 at different values of θ. (a) $\theta = -\pi/2$; (b) $\theta = 3\pi/4$; (c) $\theta = 0$. The common parameters of the graphs are $G/\kappa = 0.5, \zeta = 3$ and $\omega = 0$.

of θ and detuning Δ. Here, for simplicity we assume $\Delta_1 = \Delta_2 = \Delta$. In Figs. 3(a)–3(c), we let $\theta = 0, \pi/4, \pi/2$ and plot the spectrum versus frequency. The spectrum profile is the EIT-like two-peak shape, which is the manifestation of quantum interferences. The two-well defined resonances correspond to the two eigenvalues of the matrix $\boldsymbol{M}$,

$$\boldsymbol{M} = \begin{pmatrix} -\mathrm{i}\,\omega + i\Delta_1 + \kappa_a & \mathrm{i}\,G \\ -\mathrm{i}\,G & -\mathrm{i}\,\omega - \mathrm{i}\,\Delta_2 + \kappa_b \end{pmatrix}^{-1} \quad (11)$$

i.e., $\omega \simeq \pm\sqrt{\Delta^2 - G^2}$ if $\Delta \gg G$. As the parameter θ varies from 0 to $\pi/2$, the amplitude of the peak decreases. However, the window of the spectrum becomes wide. We have illustrated the behaviour of the spectrum for the output field of mode a (signal), the similar illustration for mode b (idler) at the output can be obtained.

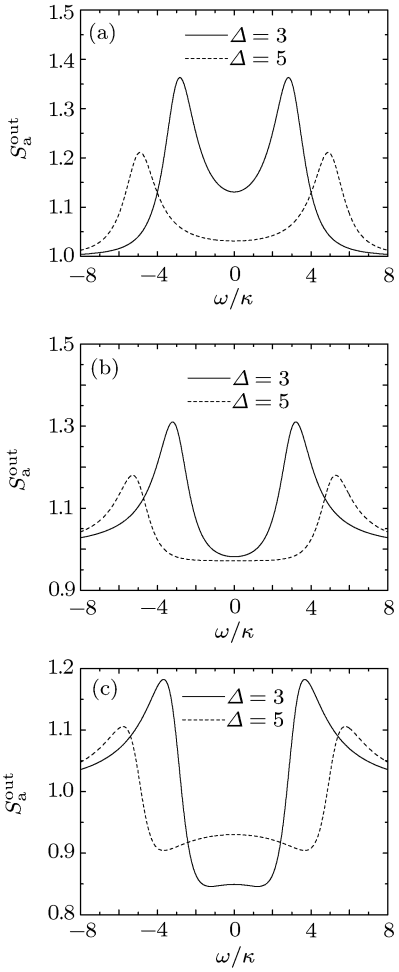


Fig. 3. The fluctuation spectra of the signal field in the output vs the frequency ω at different values of θ. (a) $\theta = 0$; (b) $\theta = \pi/4$; (c) $\theta = \pi/2$. The common parameters of the graphs are $G/\kappa = 0.5, \zeta = 3$ and detunings $\Delta/\kappa = 3, 5$.

To further demonstrate the quantum interference effect, in Fig. 4 we illustrate the quadrature phase fluctuation spectrum at the output. It is noted that this issue has not been addressed in Ref. [13]. Figure 4(a) shows the quadrature fluctuation spectrum as a function of angular frequency at $\theta = -3\pi/4$. We investigate the effect of the coupling parameter G on the quantum interferences in the output fields. When $G = 1.5$, this corresponds to the situation operated above the threshold of parametric oscillation. From the numerical illustration, it can be seen that the quadrature spectrum oscillates rapidly. The other two values of G correspond to the situations below the

threshold of parametric oscillation. In Fig. 4(b) we display the effect of changing the amount of squeezing in the input quantized fields on the quantum interferences in the output fields. This quantum statistics of the output fields clearly shows the quantum interference effects in the four-wave mixing processes.

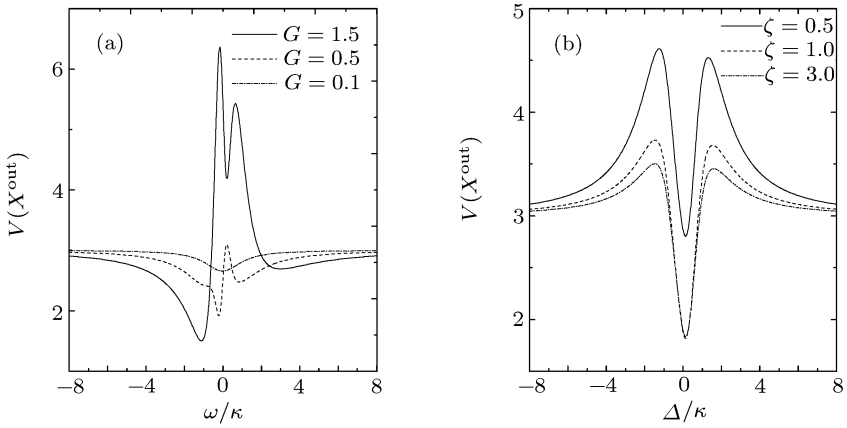


Fig. 4. Quadrature phase fluctuation spectra at the output. (a) The quadrature spectrum as a function of angular frequency at $\theta = -3\pi/4$. Other parameters are $\zeta = 3, \Delta = 0$. (b) The quadrature spectrum as a function of the detuning at $\theta = -\pi/2$. Other parameters are $\omega = 0, G/\kappa = 0.5$.

3. Summary

In summary, we have investigated the quantum interference phenomena in four-wave mixing processes inside a cavity. We demonstrate interferences in the quantum fluctuations of the output of two-mode fields when the cavity is driven by two quantized fields at the signal and the idler frequencies. These interferences depend on the phase fluctuations of the input fields and lead to mode splitting in the transmission spectra. The quadrature phase fluctuation spectra for two-mode fields are also utilized to demonstrate the interferences at the output. The novelty of this work is that we find the cross mode modulation phenomenon, i.e., the spectrum profile for one field can be controlled by varying the parameters of the other field and the interference arises not only from the input field and the produced field, but also from the two input fields themselves.

References

[1] Ficek Z and Swain S 2004 *Quantum Interference and Coherence* (Berlin: Springer-Verlag)

[2] Deng L, Payne M G and Garrett W R 2006 *Phys. Rep.* **429** 123

[3] Harris S E 1997 *Phys. Today* **50** 36

[4] Fleischhauer M, Imamoglu A and Marangos J P 2005 *Rev. Mod. Phys.* **77** 633

[5] Harris S E, Field J E and Imamoglu A 1990 *Phys. Rev. Lett.* **64** 1107

[6] Schmidt H and Imamoglu A 1996 *Opt. Lett.* **21** 1936

[7] Morigi G, Eschner J and Keitel C H 2000 *Phys. Rev. Lett.* **85** 4458

[8] Fleischhauer M and Lukin M D 2000 *Phys. Rev. Lett.* **84** 5094

[9] Li P B, Gu Y, Wang K and Gong Q H 2006 *Phys. Rev.* A **73** 032343

[10] Lukin M D and Imamoglu A 2001 *Nature* **413** 273

[11] Hu X Y, Gu Y, Gong Q H and Guo G C 2010 *Chin. Phys.* B **19** 050305

[12] Ma H, Ye C, Wei D and Zhang J 2005 *Phys. Rev. Lett.* **95** 233601

[13] Agarwal G S 2006 *Phys. Rev. Lett.* **97** 023601

[14] Zhao C Y and Tan W H 2009 *Chin. Phys.* B **18** 4143

[15] Walls D F and Milburn G J 1994 *Quantum Optics* (Berlin: Springer-Verlag)

[16] Reid M D and Walls D F 1986 *Phys. Rev.* A **34** 4929

[17] Zhang Y L, Jiang L, Sun Z R, Ding L E and Wang Z G 2003 *Chin. Phys.* **12** 0174

[18] Collett M J and Gardiner C W 1984 *Phys. Rev.* A **30** 1386

[19] Davidovich L 1996 *Rev. Mod. Phys.* **68** 127

[20] Prado F O, De Almeida A G, Moussa M H Y and Villas-Boas C J 2006 *Phys. Rev.* A **73** 043803

[21] Guzman R, Retamal J C, Solano E and Zagury N 2006 *Phys. Rev. Lett.* **96** 010502

[22] Gardiner C W and Zoller P 2000 *Quantum Noise* (Berlin: Springer-Verlag)